Journal of Chromatography A, 1217 (2010) 7055–7064

Contents lists available at ScienceDirect

Journal of Chromatography A

journal homepage: www.elsevier.com/locate/chroma

The adsorption of Naproxen enantiomers on the chiral stationary phase Whelk-O1 under reversed-phase conditions: The effect of buffer composition

Leonid Asnin[a], Krzysztof Kaczmarski[b], Georges Guiochon[c,*]

[a] Institute of Technical Chemistry, The Ural Branch of the Russian Academy of Sciences, Perm 614990, Russia
[b] Faculty of Chemistry, Rzeszów University of Technology, 35-959 Rzeszów, Poland
[c] Department of Chemistry, 552 Buehler Hall, University of Tennessee, Knoxville, TN 37996-1600, USA

ARTICLE INFO

Article history:
Received 7 June 2010
Received in revised form 29 July 2010
Accepted 26 August 2010
Available online 15 September 2010

Keywords:
Enantioselective adsorption
Chiral chromatography
Naproxen
Whelk-O1

ABSTRACT

The adsorption of the Naproxen enantiomers on the chiral stationary phase (*S,S*)-Whelk-O1 from methanol–water 80:20 (v/v) solutions modified with the addition of acetic acid or an acetic acid–sodium acetate buffer was studied using elution chromatography. Adsorption was found to be best accounted for by a two-site model assuming different retention mechanisms for the two enantiomers. Under experimental conditions causing a considerable degree of solute dissociation, strong distortion of overloaded band profiles is observed. This phenomenon is explained by the superimposition of the adsorption and the dissociation equilibria. The effect of the buffer composition on the retention is discussed and the results compared with previous ones obtained with the same system. The proposed model explains all the principal features of the adsorption of Naproxen on Whelk-O1 that were found earlier. Moreover this model applies well in a wider range of buffer concentrations, encompassing both the eluents in which solute dissociation is suppressed and those in which dissociation is significant.

1. Introduction

Ionogenic compounds, like organic acids and bases, are frequently separated in reversed-phase (RP) chromatography, a mode of chromatography that exploits molecular adsorption, not ion-exchange. It is recommended to perform such separations under experimental conditions that impede the dissociation of the target analytes by addition of a proper buffer system. However, the complete suppression of the analyte ionization cannot be achieved in a number of cases. Then the secondary equilibrium of analyte dissociation affects the elution process, both under non-linear chromatography conditions [1–3] and even under linear [4–6]. The nature and composition of a buffer system, which are the main factors controlling the mobile phase pH, significantly influence the separation of ionogenic analytes. In a variety of ion-exchange processes, this phenomenon was a topic of continuous and comprehensive investigations [7–9]. In chromatography on uncharged stationary phases, Horvath, Melander and Molnar seem to have been the first to address the issue of the elution of ionizable analytes in terms of retention mechanisms [10]. Later, Kazakevich described a solution of the mass balance equation for a basic analyte in RPLC, taking into account the dissociation equilibrium and used this solution to analyse the effect of the buffer concentration on the retention of infinitely diluted samples [6].

Fornstedt et al. [11,12] reported that the effect of the mobile phase pH on the retention of β-blockers on an immobilized cellulase is controlled by the influence of the pH on the activity of different types of adsorption sites, demonstrating that, due to the heterogeneity of the surface of the stationary phases, the simple theory of chromatography cannot, generally, explain the adsorption mechanism, even under linear chromatography conditions and let alone the elution of overloaded bands. In a series of works [1–3], Gritti et al. developed an approach to describe the adsorption of acidic and basic solutes on C_{18}-bonded silica from buffered mobile phases. This approach combines the multi (usually, bi) Langmuir adsorption isotherm and the equilibrium between the neutral and the ionized forms of the analyte. Although the problem of chromatography of ionizable substances on uncharged stationary phases appears to be now well understood, there is still room to improve our knowledge of this field, particularly in chiral chromatography, a field in which authors tend to confine themselves mostly to report the results of empirical observations of the effect of the mobile phase pH and the buffer system composition on the elution characteristics under linear conditions (see, for instance, [13,14]), without attempting to provide any rational explanations.

There are only a few exceptions to this line of investigations. Besides the case mentioned above of the adsorption of chiral analytes on immobilized proteins [11,12,15], we published recently a series of reports aiming at elucidating the complexity of the

* Corresponding author. Tel.: +1 865 974 0733; fax: +1 865 974 2667.
E-mail address: guiochon@utk.edu (G. Guiochon).

0021-9673/$ – see front matter © 2010 Elsevier B.V. All rights reserved.
doi:10.1016/j.chroma.2010.08.073

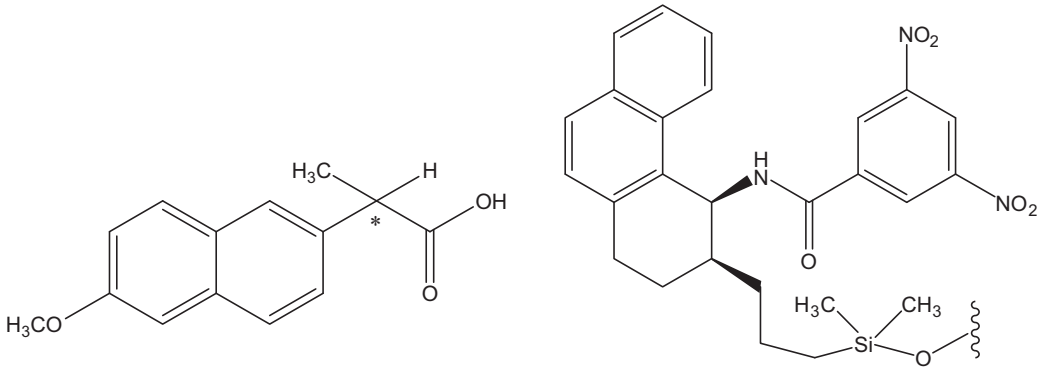

Naproxen (*S,S*)-Whelk-O1

Fig. 1. Naproxen (the "star" symbol shows the location of the chiral center) and (*S,S*)-Whelk-O1 chiral selector.

processes occurring in buffered media that affect the elution of overloaded samples in chiral systems, based on the separation of the enantiomers of Naproxen on the Whelk-O1 CSP (Fig. 1). This adsorption system was chosen because the chiral recognition mechanism involved was previously and comprehensively studied [16–19], which greatly facilitates a detailed discussion of the adsorption equilibrium. We showed earlier that moderate variations of the mobile phase composition influence the shape of the peaks of the Naproxen enantiomers on a Whelk-O1 CSP and suggested that the methanol–water ratio was mostly responsible for changes in the retention mechanism [20]. Then, we found that the methanol concentration affects the band profiles because it controls the mobile phase pH and the degree of dissociation of the analyte [21]. We also observed (but without exploring further) that the concentration of the mobile phase buffer also determines the elution profile [22]. Later work [23] investigated the thermodynamics and mass transfer kinetics of the adsorption of the Naproxen enantiomers on Whelk-O1 at constant mobile phase composition. However, the effect of the buffer concentration on the adsorption equilibrium in the system studied remains unclear and the main objective of this work is to clarify it. A shortcoming of earlier work is the relatively narrow range of concentrations studied, which prevents the distortion of band profiles from being sufficiently pronounced. In this work, a fivefold wider concentration range was studied.

2. Theory

2.1. Adsorption isotherm models for weak electrolyte solutes

A weak electrolyte exists in solutions in two forms, dissociated (ionic) and undissociated (neutral). The total electrolyte concentration c_T is the sum of the individual concentrations of the ionic (c_I) and the neutral (c_N) molecules. The total uptake of solute, q_T, is the sum of the amounts of the two forms adsorbed

$$q_T = q_I + q_N \tag{1}$$

If the adsorption of the charged and the neutral species can be considered as independent, the partial uptakes are functions of the equilibrium concentrations of either species, that is of $q_I(c_I)$ and $q_N(c_N)$, respectively. In the case of competitive adsorption, the partial adsorption isotherms depend on the concentrations of both species, $q_I(c_I, c_N)$ and $q_N(c_I, c_N)$. The ratio between the concentrations of the ionic and neutral forms of an analyte in the bulk solution is determined by its dissociation constant K_a (which in turn depends on the nature of the solvent and solute, on the temperature and the pressure) and by the composition of the solution. This ratio can be computed by solving the set of ionic equilibrium equations for the liquid phase components, supplemented with the equations of mass conservation and solution electroneutrality. In principle, this set of equations has to be considered along with Eq. (1) in order to derive the function $q_T(c_T)$. However, in multicomponent buffer mixtures the complete set of equations lacks a solution that could be expressed in an explicit form. Previous authors [1–3] proposed an approach to overcome this inconvenience. It consists in solving numerically the set of ionic equilibrium equations for the dissociation degree $\alpha = c_I/c_T$ as a function of the analyte concentration in the whole range of interest. Furthermore, the calculated data $\alpha(c_T)$ are approximated with a suitable, usually a polynomial, function. The adsorption isotherm (1) can then be expressed as a function of c_T for $c_I = c_T\alpha$ and $c_N = c_T(1-\alpha)$. Consequently, in the case of the independent adsorption of the charged and the neutral species, $q_I(c_I) = q_I(c_T\alpha)$ and $q_N(c_N) = q_N(c_T[1-\alpha])$. Only independent adsorption will be discussed below for the sake of simplicity. The following consideration can be easily extended to the competitive case as shown, for example, in Ref. [2].

The practical use of Eq. (1) requires knowledge of the adsorption isotherms of the neutral and the ionic species. A common adsorption model widely used in solid–liquid equilibria is the Langmuir one. This model assumes that the solid surface bears a finite number of identical adsorption sites and that the adsorbed particles do not interact with each other on the surface. The equation relating the adsorbed amount q to the equilibrium bulk concentration c of an adsorptive is

$$q = \frac{q^* bc}{1 + bc} \tag{2}$$

where q^* is the saturation capacity of the stationary phase and b the adsorption equilibrium constant. The phenomenon of lateral interactions on the surface is taken into account in the Moreau isotherm [24]:

$$q = \frac{q^*(bc + I(bc)^2)}{1 + 2bc + I(bc)^2} \tag{3}$$

The adsorbate–adsorbate interaction parameter I is larger than 1 if these interactions are attractive and it is between 0 and 1 if the interactions are repulsive.

For chemically bonded stationary phases, it was found that there can be more than one type of adsorption sites [2,25–28]. For example, a quinidine carbamate CSP exhibits two distinct types of adsorption sites with respect to chiral arylcarbinols. These sites correspond probably to different conformations of the bonded chiral selectors [27,28]. Assuming independent adsorption of a solute on the different types of adsorption sites, the overall equilibrium

isotherm is the sum of the respective local isotherms:

$$q = \sum_{i=1}^{n} T_i(\mathbf{P}_i, c) \tag{4}$$

where T_i is a function of the local adsorption isotherm for the sites of type i, $\mathbf{P}_i$ being a vector of the isotherm parameters. Most often, the Langmuir model is chosen as the T-function, but also other isotherm expressions, such as the Moreau [29] or the Jovanovich–Freundlich [30] models, have been used.

The isotherm models developed for non-ionic molecules like those shown in Eqs. (2) and (3) can be used to describe the adsorption of charged species. Such an approach was successfully applied by Gritti and Guiochon to explain the retention of iogenic organic acids and bases in RPLC [1–3]. It must be kept in mind, however, that the equilibrium constant in this case relates to the difference of the electrochemical potentials of a charged particle in the bulk solution and in the adsorbed phase rather than to that of chemical potentials (the electrochemical potential includes an electrostatic energy term associated with the charge of an ion). Another concept considers the formation of a double layer at the solid–liquid interface and electrostatic interactions between the surface and the charged analyte, leading to isotherms of ion adsorption like those of Frumkin [31] or Ståhlberg [32,33]. These isotherms are implicit, thus their use in the simulation of band profiles generates considerable mathematical difficulties. Therefore the former (phenomenological as to charged species) approach was employed to represent the adsorption of ions in the present study.

2.2. Ionic equilibria in solutions

Since the evaluation of the dissociation degree is an important part of this work, it is pertinent to give a brief account of the theory lying behind these calculations. Naproxen (HNp) is a weak acid that dissociates into the Naproxen-anion (Np^-) and a hydrogen-cation according to the following equation:

$$HNp \rightleftharpoons H^+ + Np^- \tag{5}$$

with the dissociation constant

$$K_N = \frac{[H^+][Np^-]\gamma_H\gamma_{Np}}{[HNp]\gamma_{HNp}} \tag{6}$$

where the equilibrium concentrations are placed between square brackets. The symbol γ designates the activity coefficient and the subscript indices H, Np, and HNp stand for the proton, the Naproxen-anion, and the neutral acid, respectively.

The mobile phases studied here are buffer solutions that contain the buffer (acetic) acid and occasionally the buffer salt (sodium acetate). The equilibrium equation for the dissociation of acetic acid (HOAc) is

$$HOAc \rightleftharpoons H^+ + OAc^- \tag{7}$$

with

$$K_A = \frac{[H^+][OAc^-]\gamma_H\gamma_{OAc}}{[HOAc]\gamma_{HOAc}} \tag{8}$$

where the subscripts OAc and HOAc stand for the acetate-anion and the neutral acid, respectively. In a solution, another equilibrium takes place, the autoprotolysis of the solvent:

$$HS \rightleftharpoons H^+ + S^- \tag{9}$$

with the autoprotolysis constant:

$$K_S = [H^+][S^-]\gamma_H\gamma_S \tag{10}$$

Actually, the solvent is binary and both its components dissociate. However, as we use in the calculation the effective autoprotolysis constant of the medium, we may approximate the virtual complex scheme of the autoprotolysis of the methanol–water mixture with a single component equilibrium (10)[34], assuming $\gamma_S = \gamma_{OH}$. The values of the equilibrium constants pK_N, pK_A, and pK_S in a 80:20 (v/v) methanol–water at ambient temperature are 6.58 [35], 6.49 [34], and 14.63 [34], respectively.

Eqs. (6), (8) and (10) supplemented with the equations of mass conservation (11)–(13) and of electroneutrality (14) make a closed set of equations, whose solution with respect to $[Np^-]$ gives the dissociation degree of Naproxen as a function of c_T once the activity coefficients are defined. In the equations below, c_{HOAc} and c_{NaOAc} are the total concentrations of acetic acid and sodium acetate, respectively:

$$c_{HNp} = c_T = [HNp] + [Np^-] \tag{11}$$

$$c_{HOAc} + c_{NaOAc} = [HOAc] + [OAc^-] \tag{12}$$

$$c_{NaOAc} = [Na^+] \tag{13}$$

$$[Np^-] + [OAc^-] + [S^-] = [Na^+] + [H^+] \tag{14}$$

We follow the usual practice of assuming that the activity coefficients of undissociated molecules are equal to 1. Those of the ions are found by means of the Debay–Hückel equation

$$\log \gamma_i = -\frac{Az_i^2\sqrt{I}}{1 + Ba_{0,i}\sqrt{I}} \tag{15}$$

where z_i is the charge of the ion, I is the ionic strength of the solution, A and B are two parameters that depend on the temperature and the dielectric constant, ε, of the solvent, and $a_{0,i}$ is the ion-size parameter. The latter quantity was assumed to be equal to 4.56 [34] for all ions but the Naproxen-anion, for which the value of 6.3 recommended for arenecarboxylate ions [36] was taken. A and B are written [34]:

$$A = \frac{1.8246 \times 10^6}{(\varepsilon T)^{1.5}} \tag{16}$$

$$A = \frac{50.29}{(\varepsilon T)^{0.5}} \tag{17}$$

The value of ε, which is needed to evaluate these parameters is 43.7 in a 80:20 (v/v) methanol–water, at 27 °C [37].

The ionic strength, by definition, is given by the summation over all the ions present in solution at equilibrium:

$$I = \sum_i z_i^2[\mathrm{Ion}_i] \tag{18}$$

As one does not know the equilibrium concentration of most ions until the problem is solved, one should use an iterative procedure to evaluate the ionic composition, starting from an initial guess for the ionic strength [38]. This procedure is justified by a good agreement between the predicted and the measured pH of the investigated buffer solutions, the difference being less than 1.5%. In performing this test, it was taken into account that the pH found with a potentiometric system standardized with aqueous buffers, ${}^s_w\mathrm{pH}$, is the apparent quantity that relates to the value expressed in a scale for the given hydro-organic solvent, ${}^s_s\mathrm{pH}$, as [39]

$${}^s_s\mathrm{pH} = {}^s_w\mathrm{pH} - \delta \tag{19}$$

where the δ parameter is constant for a given electrode system in a certain solvent. It is 0.045 when determined with the glass electrode in the methanol–water mixture of interest [40].

Finally, we need to mention that the proposed model of ionic equilibria in solution does not consider the exchange of hydrogen-cations and buffer ions with the solid phase, which is a fundamental assumption questioning the adequacy of the evaluation of the $\alpha(c_T)$ dependence. This assumption cannot be avoided due to the lack of

information concerning the distribution of these species between the mobile and the stationary phases within the solute band. When the solute band migrates along the column, its passage disturbs the local equilibrium achieved between the two phases. Then, the ion concentrations may differ from those predicted from Eqs. (5), (7) and (9), due to the ion-exchange and dissociation processes taking place on the surface, which can release or consume ions to or from the bulk solution. On the other hand, previous results [20,23] allow us to suppose that the involvement of the surface in regulating the mobile phase pH and the buffer concentration is minor. Indeed, the residual silanols are well shielded by the grafted organic layer, which itself does not contain any strong acidic or basic functionalities.

3. Experimental

3.1. Apparatus

All experiments were carried out using a HP 1090 Series II liquid chromatograph (Agilent Technologies, Palo Alto, CA), equipped with a multisolvent delivery system, an automatic injector, a column thermostat, a DAD detector, a HP 1037A refractive index detector (used only for hold-up volume determination with isotopically labeled methanol) and a HP Chemstation data acquisition system. The extra-column volume measured from the autosampler to the DAD detector in the system with a zero-volume connector installed in place of the chromatographic column was 0.032 ml. All the retention data were corrected for this contribution.

The measurements of the ${}^{s}_{w}$pH of the mobile phase during elution of the analyte samples were performed with a flow through micro-pH-electrode (Lazar Research Laboratories Inc., Los Angeles, CA) connected to the outlet of the DAD detector. The pH-electrode was calibrated with two standard aqueous solutions at pH = 4.00 and 9.00. The pH measuring cell had a volume of 0.020 ml. The volume of the flow path between the detector and the cell was 0.168 ml. This value was derived from the retention delay between the maxima of the DAD response and the pH-electrode response recorded without the column after the injection of 8.5 g/L (*S*)-Naproxen with mobile phase methanol–water, 90:10 (v/v). All the respective data were corrected for this contribution.

3.2. Chromatographic column

A 250 mm × 4.6 mm column was used, packed with ~2.5 g of non-endcapped (3*R*,4*S*)-Whelk-O1 material, 5 μm particle size, 100 Å pore size, spherical silica (trade name (*S*,*S*)-Whelk-O1). It was purchased from Regis Technologies (Morton Grove, IL, USA). The surface area of the silica support was 200 m^2/g and its internal porosity 0.5 cm^3/g, as reported by the manufacturer. This CSP was found to be prone to gradual deterioration when in contact with acidic aqueous solutions at elevated temperatures [20]. In the current study, the mobile phase composition and the temperature were kept remote from the risk region to avoid damage to the column.

3.3. Chemicals

The components of the mobile phases, HPLC grade water, methanol, and acetic acid, were purchased from Fisher Scientific (Fair Lawn, NJ, USA). Deuterated methanol (99.8 %) used for hold-up volume measurements was from Alfa Aesar (Ward Hill, MA, USA). (*S*)-Naproxen was from Cayman Chemicals and (*R*)-Naproxen was from Sigma–Aldrich (St. Louis, MO, USA). Their purity was controlled by HPLC. The contamination of each enantiomer by its optical antipode was found to be less than 0.2 and 0.5 % for (*S*)- and (*R*)-enantiomer, respectively. No other UV-detectable impurities were found.

Table 1
Mobile phases.

Mobile phase code	Mobile phase	${}^{s}_{w}$pH	${}^{s}_{s}$pH
A1	0.01 M CH_3COOH	4.25	4.20
AN1	0.01 M CH_3COOH–0.01 M CH_3COONa	6.35	6.30
AN3	0.03 M CH_3COOH–0.03 M CH_3COONa	6.35	6.30

3.4. Mobile phases

The mobile phases were solutions of acetic acid or acetic acid-sodium acetate buffers in a methanol–water (80:20, v/v) mixture (Table 1). The solutions prepared were degassed by ultrasonication for 5 min, followed by the measurement of the ${}^{s}_{w}$pH with a glass electrode calibrated against aqueous buffers, using the American pH II pH-meter (Baxter Scientific, Stone Mountain, GA).

It seems appropriate to note that the preparation of the mobile phase used in this study differs from the one used for the same purpose in an earlier work [20], in which an aqueous buffer of a known composition was mixed with methanol in the required proportions.

3.5. Procedures

3.5.1. Measurement of the hold-up volume

According to Knox and Kaliszan [41] the retention volume of a pulse of an isotopically labeled solvent eluted by the same non-labeled solvent is equal to the void or hold-up volume of the column, V_0. Measurements were made at a temperature of 27 °C, using pure methanol as the mobile phase and deuterated methanol as the tracer. The tracer concentration was 1 vol.%, the sample size was 2 μl.

3.5.2. Determination of the adsorption isotherms by the pulse method

The adsorption equilibrium of the Naproxen enantiomers was measured by a modified Glueckauf method [42,43], in which sample pulses of increasing sizes are injected after equilibration of the column with the mobile phase. To derive the adsorption isotherm, the following equation was applied:

$$\frac{dq(c)}{dc} = \frac{(V_R(c) - V_0)}{V_a} = V'_R(c) \quad (20)$$

where V_a is the volume of the stationary phase, $V_R(c)$ is the retention volume of the apex of the peak, corresponding to the mobile phase concentration of an adsorbate at the apex, $q(c)$ being the adsorbed amount of solute at equilibrium with this concentration c. Thus, the retention time of each peak gives one point on the $V'_R(c)$ versus c plot. By repeating the procedure while progressively increasing the sample concentration, the set of data $V'_R(c)$ versus c is obtained within the concentration range of interest. The amount adsorbed $q(c)$ is obtained by integration of the area under the function $dq(c)/dc$ from 0 to c.

The experiments were carried out at 27 °C, at a flow rate of 1 ml/min. The sample volume was 100 μl, the sample concentration was increased from 0.2 to 43.4 mM. Before beginning the measurements the column was flushed with the mobile phase for no less than 1 h, to achieve equilibrium conditions. Conversion of the detector signal to the concentration profile was fulfilled with help of the calibration curve determined by means of a self-calibrating procedure [27] performed simultaneously on two chromatograms, with the highest and one of intermediate injected amounts.

3.5.3. Determination of the adsorption isotherms by the inverse method

The inverse method provides the numerical coefficients of a preset isotherm model through an optimization procedure that minimizes the distance between an experimental overloaded band profile and the profile calculated with a suitable model of chromatography [44]. The equilibrium-dispersive (ED) model of chromatography [44] was used in these calculations. The mass balance equation for this model is

$$\frac{\partial c(z,t)}{\partial t} + \left(\frac{1-\epsilon}{\epsilon}\right)\frac{\partial q(z,t)}{\partial t} + u\frac{\partial c(z,t)}{\partial z} = D_a\frac{\partial^2 c(z,t)}{\partial z^2} \quad (21)$$

where z is the abscissa along the column, t the time, u the mobile phase linear velocity, and ϵ the total porosity of the column. D_a is the apparent axial dispersion coefficient. Its value was determined according to the procedure described in [45], which consists in finding the D_a value that gives a calculated chromatographic peak having the same slope for its steepest flank as the experimental profile. A short discussion of this approach was given earlier [46].

The calculation of a numerical solution of a partial differential equation requires selection of the initial and boundary conditions. The following conditions are used to solve Eq. (21).

- The initial conditions are $c(z,t)=0$ and $q(z,t)=0$. They state that at $t=0$, the column is in equilibrium with the pure mobile phase.
- The Danckwerts-type [47] boundary condition at the column inlet (at $t>0$ and $z=0$) is given by

$$uc(0,t) = uc_0' + \epsilon D_a\cdot\frac{\partial c}{\partial z}$$
$$c_0' = \begin{cases} c_0 & \text{if} \quad 0 < t < t_p \\ 0 & \text{if} \quad t_p < t \end{cases} \quad (22)$$

  where t_p is the duration of the injection and the subscript 0 indicates an "inlet value".
- The boundary condition at the column outlet (at $t>0$ and $z=L$) is

$$\frac{\partial c}{\partial z} = 0 \quad (23)$$

These conditions correspond to the injection of a rectangular plug of sample with concentration c_0 instead of the experimental injection profile $c_0(t)$ that can be recorded in the system without column. Preliminary numerical calculations showed that both approaches result in similar chromatograms, with a difference in the retention times of less than 1%. In the same time, the rectangular plug assumption allows faster computation.

The optimization procedure used to find the best fitting isotherm parameters [48] was performed for each enantiomer simultaneously, with the three elution profiles obtained with the three mobile phases studied. The chromatograms corresponding to the highest sample concentration (43.4 mM) were used for these calculations. This multiprofile technique allows one to reduce the number of adjustable parameters and, consequently, provides an improvement of the robustness of the procedure. The optimization algorithm was that of Marquardt, modified by Fletcher [49]. During the optimization runs, the mass balance equation for each peak was integrated numerically with the Rouchon method modified for the multiprofile problem [48].

3.6. Measurement of ${}^{s}_{w}$pH profiles

The ${}^{s}_{w}$pH profiles were measured using the experimental setup described in Section 3.1. The flow rate was kept constant at 0.2 ml/min, as recommended in [50]. The sample concentration was 34.7 mM for both enantiomers, the sample volume being 100 μL. The DAD detector response was recorded simultaneously.

4. Results and discussion

Two common methods are used to derive adsorption equilibrium information from elution profiles, the pulse method (also known as the Glueckauf method) and the inverse method [44]. Both methods were applied to analyse the experimental data presented in Fig. 2.

4.1. Glueckauf method

The Glueckauf method is based on the ideal model of chromatography, implying (i) instantaneous equilibrium in the column and (ii) a negligible influence of the mass transfer kinetics on the dispersion of the chromatographic band. There is a further assumption, usually omitted, the relevancy of which will be made clearer later. It is the chemical integrity of the eluted component. Indeed, the retention equation used in the Glueckauf method (Eq. (20)) is not valid if the eluted component undergoes any chemical transformation. A good indication that an experimental system meets the conditions of the ideal model is when the diffuse fronts of samples of increasing sizes nearly coincide [51]. The data in Fig. 2 show that this condition is acceptably satisfied only for the 0.01 M acetic acid solution (some discrepancy found in Fig. 3d can be ascribed to minor, casual deviations from equilibrium in the column). For the eluents modified by the addition of sodium acetate (Fig. 2b, c, e, and f), the profiles progressively shift from one to the other when the injected amount increases.

The fundamental difference between the buffered (AN1 and AN3) and unbuffered (A1) mobile phases lies in the fact that the dissociation of acid analytes is suppressed in the latter case (Fig. 3). It is logical then to explain the observed phenomenon by the coexistence of the two solute species in the buffered solutions, the neutral molecules and the ions. The chromatographic bands of the two species migrate along the column at different velocities but the bands are bound by the dissociation equilibrium. The total retention in such a system is a function of the partial adsorption isotherms of each species and of the pH [6]. Both the partial adsorption isotherms and the mobile phase pH are functions of the overall bulk solute concentration and of the dissociation equilibrium constant. This can explain why the c_T versus V_R curves for different sample sizes do not coincide. The higher the sample size, the higher the perturbation of the pH in the solute band. Consequently, chromatographic bands of different samples travel under different ionic conditions and their elution curves cannot be similar. Thus, the requirement of chemical integrity is not met, which has some visible consequences.

Nevertheless, we can formally apply the Glueckauf method to derive adsorption isotherms if we bear in mind that the functions obtained are apparent, not true isotherms. Fig. 4 shows plots of the reduced retention volume V_R' versus the solute concentration at the peak apex, $c_{apex,T}$, and the two respective apparent adsorption isotherms calculated. Note that the $V_R'(c)$-functions for the mobile phases A1 and AN1 tend to approach each other, and actually do so for (*R*)-Naproxen because the buffer capacity of the solvent AN1 is not large enough to prevent the local acidification of the mobile phase when the solute concentration becomes higher than the buffer concentration. This is not the case for the eluent AN3, which has a threefold higher buffer content. An illustration of the effect of the buffer capacity on the local ${}^{s}_{w}$pH of the mobile phase is shown in Fig. 5. The amplitude of the ${}^{s}_{w}$pH perturbation is four times higher for the less buffered solvent.

Plots of the reduced retention volumes in buffered mobile phases have inflection and extremum points. The positions of these peculiar points do not match for the two enantiomers, suggesting that the effect of enantioselective adsorption is superimposed to the effect of the dissociation equilibrium. The occurrence of extremum points on the curves indicates the existence of inflection

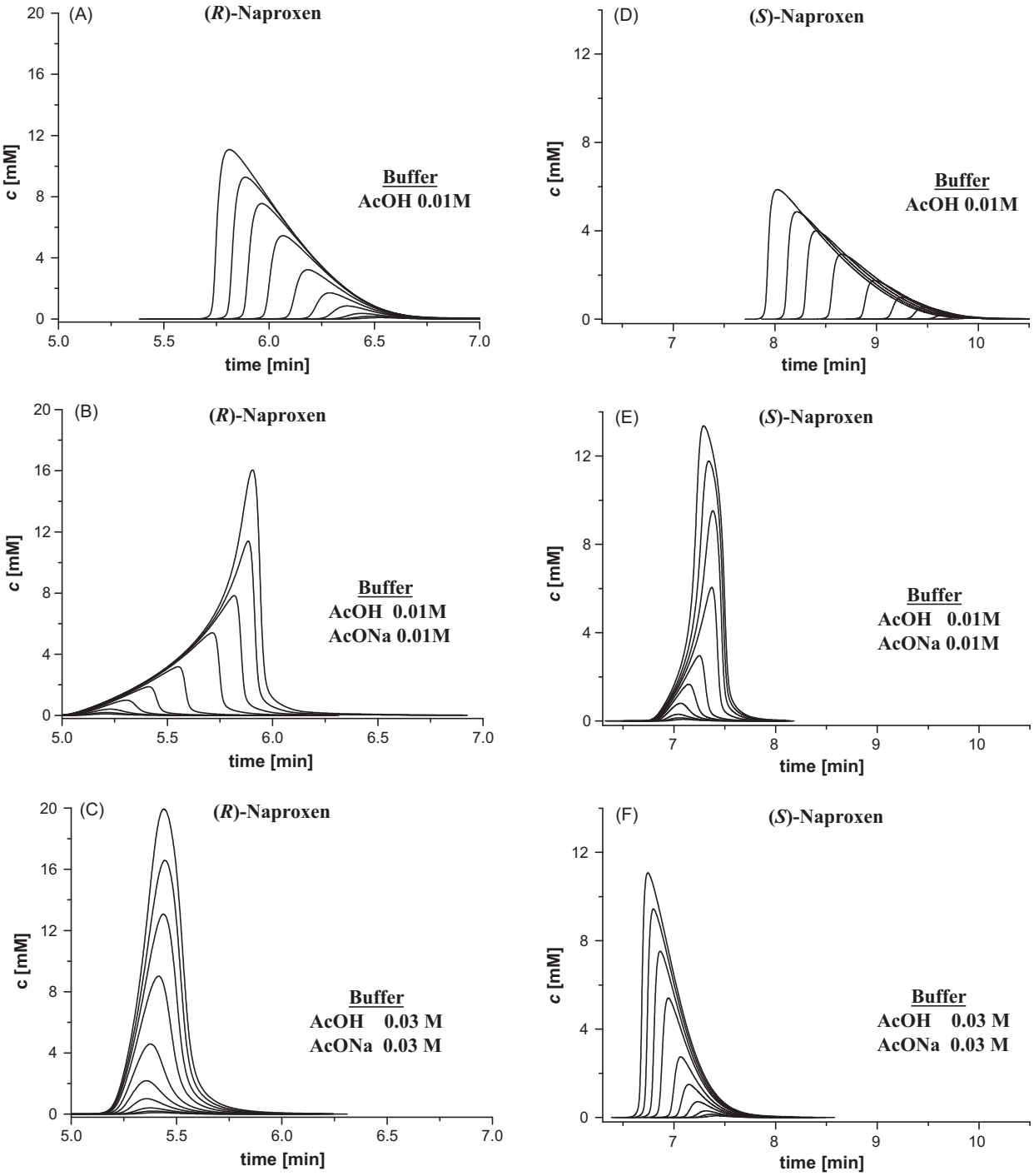

Fig. 2. Illustration of the effect of buffer composition and the sample size on elution profiles of Naproxen enantiomers. The composition of buffer system is shown on the graphs using designation AcOH and AcONa for acetic acid and sodium acetate, respectively. Sample volume 100 μl; sample concentrations: 0.22, 0.43, 0.87, 2.17, 4.34, 8.69, 17.4, 26.1, 34.7, 43.4 mM.

points on the total adsorption isotherms. Those measured with the acidic eluent A1 go higher than isotherms for the buffered eluents (Fig. 4), consistent with a stronger retention of both enantiomers in the former mobile phase (see Fig. 2). The difference between the total (apparent) amount of (*S*)-Naproxen adsorbed from solutions AN1 and AN3 is minor within a large part of the concentration range investigated. It is larger in the case of (*R*)-Naproxen for c_T >10 mM. These findings are hard to explain due to the ambiguity of the results. Although being formally ascribed to a single component, actually the data belong to a reversible binary system. This obstacle can be overcome by analyzing otherwise the overloaded band profiles. For this purpose, we calculated numerically band profiles using the combination of adsorption models and the dissociation of the analyte [1–3]. The results obtained are described in the next section.

4.2. The inverse method

The inverse method consists in adjusting the numerical coefficients of an isotherm model to minimize the differences between the band profile recorded for a compound and the profile calculated from this isotherm by numerical integration of the mass balance,

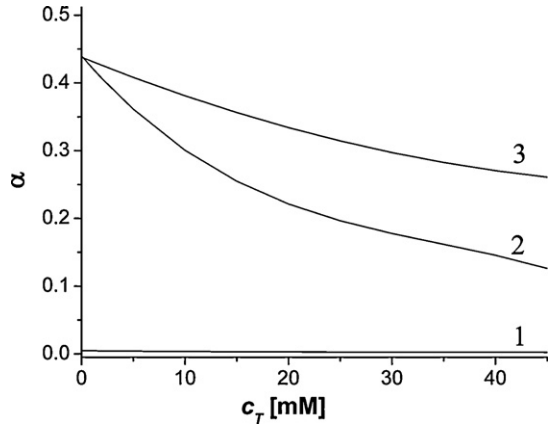

Fig. 3. Dissociation degree of Naproxen as a function of its concentration for eluents A1 (1), AN1 (2), and AN3 (3); see Table 1 for explanation.

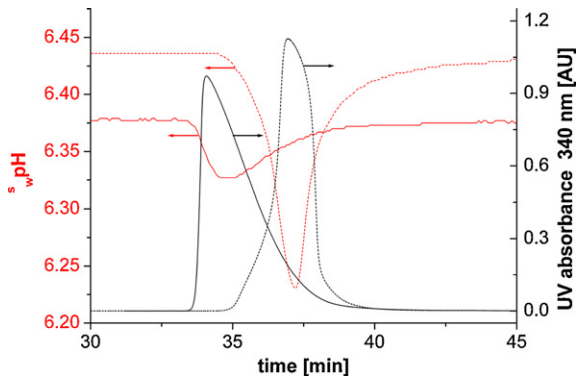

Fig. 5. $^{s}_{w}$pH profiles (red) and DAD signal profiles (black) of (*S*)-Naproxen recorded with mobile phases AN1 (dashed lines) and AN3 (solid lines). Sample volume 100 μl; sample concentration 43.4 mM. Note the simultaneous beginning of respective $^{s}_{w}$pH and elution profiles. (For interpretation of the references to color in this figure legend, the reader is referred to the web version of the article.)

under the same experimental conditions. This method requires the *a priory* choice of an isotherm model and the use of an optimization algorithm. The choice of the isotherm model depends on the shape of the recorded band profile and on the adsorption isotherm previously measured. Unfortunately, this additional information is uncertain in the case of compounds that may dissociate in the mobile phase. As shown above, band profiles eluted under such experimental conditions are the convolution of the effects of adsorption and dissociation. Therefore, it may be difficult to relate the profile shape and an adsorption model. However, it was shown in the theory section that the total adsorption isotherm can be approximated by the weighed sum of the partial isotherms of the neutral and the ionized species, the weight coefficients depending

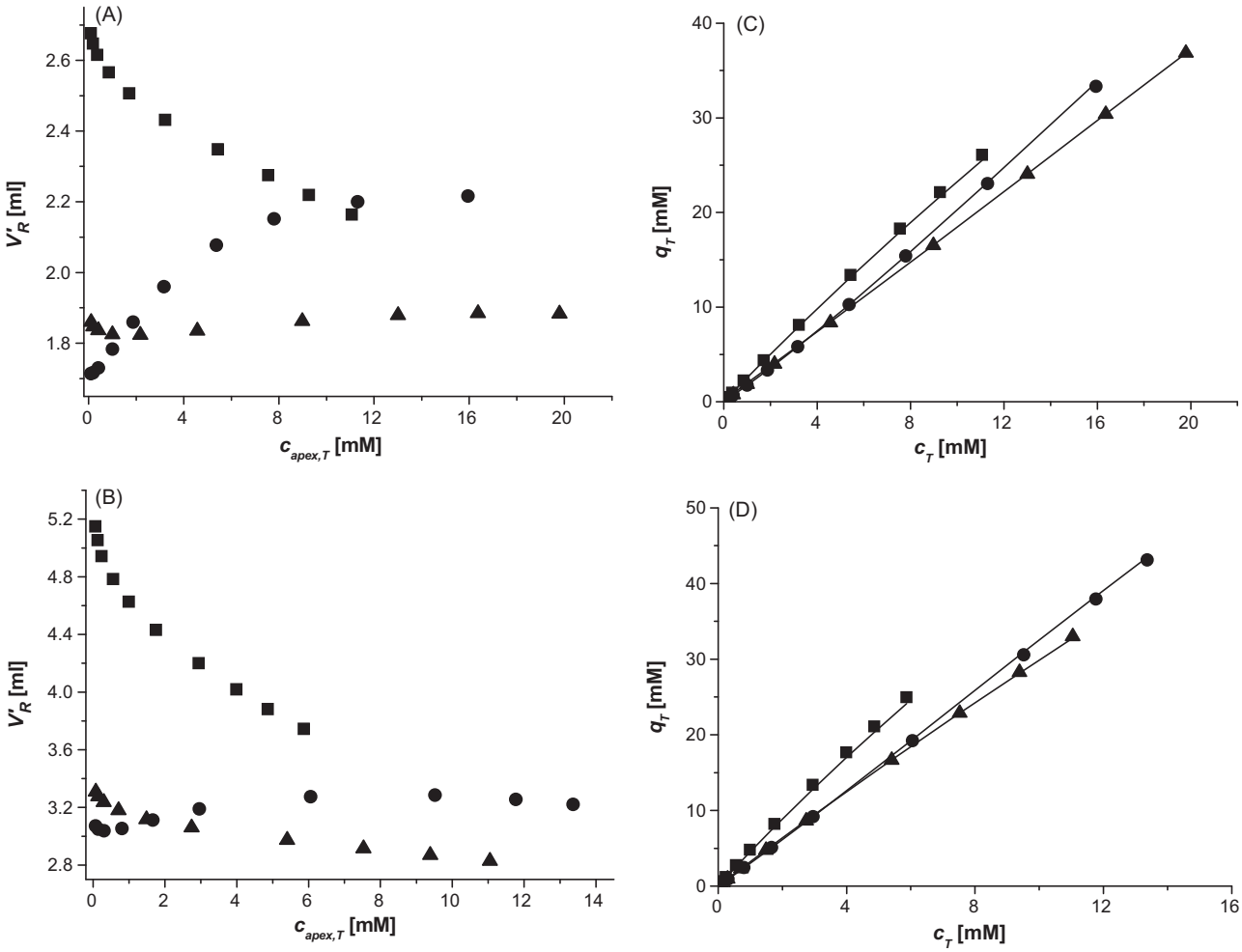

Fig. 4. Dependence of the reduced retention volume on the concentration at the apex of a peak (a and b) and adsorption isotherms (c and d) of (*R*)-Naproxen (a and c) and (*S*)-Naproxen (b and d). Square, circle, and triangle symbols represent data for mobile phases A1, AN1, and AN3, respectively. In graphs c and d, symbols shows data obtained by the Glueckauf method, lines are the adsorption isotherms derived by the inverse method.

on the dissociation degree. Common adsorption models like the Langmuir or the Moreau models can be used as approximations of the partial isotherms. The accuracy of the results thus obtained depends both on the adequacy of the isotherm model chosen and on the accuracy and precision of the estimate of the dissociation degree.

4.2.1. Selection of an isotherm model

The general requirements for an adsorption model are: (1) the same model must be used for a given enantiomer in all eluents used but a different model may be used for the two enantiomers; (2) the surface density of the selective adsorption sites must be the same over the entire range of buffer concentrations studied, only the strength of the solute-site interactions may vary as a function of the buffer composition; physically, this also means that a change in the salt concentration or in the pH does not result in the exclusion of the chiral selectors from adsorption model.

Taking into account these restrictions, a number of isotherm models were designed according to Eq. (4). The dissociation equilibrium was directly implemented into these models by accepting that $c_T(1-\alpha)$ and $c_T\alpha$ be the bulk concentrations of the molecular Naproxen and the Naproxen-anion, respectively. The dissociation degree was permitted to be $\alpha = 0$ in mobile phase A1. Two- and three-site models were considered, either including or excluding a term for anion adsorption. The Langmuir, Moreau, or Langmuir–Freundlich equations [44] were used as local isotherms. All possible combinations of the Langmuir and the Moreau terms in the frameworks of the two-site models and several combinations in the frameworks of the three-site model were tested. The Langmuir–Freundlich function was combined only with the Langmuir one. Both the Langmuir and Moreau models were applied to describe the retention of anions. The primary rejection criteria was visual. Those models that could not predict essential features of the chromatograms (for example, gave a steep front instead of a diffuse one) were not considered further. Also the models that led to meaningless values of the isotherm parameters, were excluded. So, it was found that an anion adsorption term was not necessary in the tri-Langmuir model. The best-fit adsorption coefficient for anions was a few orders of magnitude lower than the computation error. The use of an anion term in the two-term isotherm equations led to results with poorer statistic indicators than the same equations considering only neutral acid adsorption. It was concluded that the retention of anionic species does not play a significant role in the adsorption of Naproxen under the selected experimental conditions. This may not be the case for solvents with lower methanol concentrations [22].

The remaining models were ordered by value of the difference between the best-fit and the experimental band profiles. The best model assumes Langmuir–Moreau adsorption for the less retained (*R*)-enantiomer and bi-Langmuir adsorption for the (*S*)-enantiomer, as given by the following equations:

1. for (*R*)-Naproxen:

$$q = \frac{q_1^*(b_1 c_T(1-\alpha) + I[b_1 c_T(1-\alpha)]^2)}{1 + 2b_1 c_T(1-\alpha) + I[b_1 c_T(1-\alpha)]^2} + \frac{q_2^* b_2 c_T(1-\alpha)}{1 + b_2 c_T(1-\alpha)} \quad (24)$$

2. for (*S*)-Naproxen:

$$q = \frac{q_1^* b_1 c_T(1-\alpha)}{1 + b_1 c_T(1-\alpha)} + \frac{q_2^* b_2 c_T(1-\alpha)}{1 + b_2 c_T(1-\alpha)} \quad (25)$$

In general, we suppose $q^*_{1(2)}(R) \neq q^*_{1(2)}(S)$ and $b_{1(2)}(R) \neq b_{1(2)}(S)$. Respective specifying indices are omitted in the equations above for the sake of simplicity.

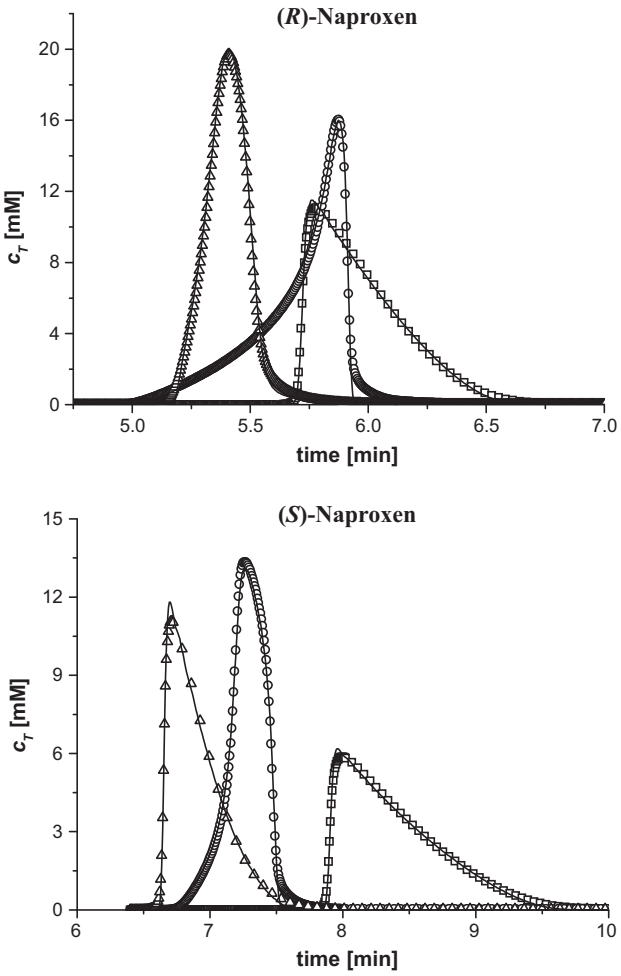

Fig. 6. Comparison of the experimental chromatograms of (*R*)- and (*S*)-Naproxen (symbols) and those calculated using the inverse method (lines). Square, circle, and triangle symbols represent data for mobile phases A1, AN1, and AN3, respectively. Sample concentration is 43.4 mM for all chromatograms.

Fig. 6 compares the experimental band profiles and those calculated using Eqs. (24) and (25), with the best coefficients given in Table 2. The inverse method procedure was performed for each enantiomer on the three profiles simultaneously. Since the saturation capacities, q_1^* and q_2^*, are assumed to be independent of the mobile phase composition, they should be the same for each profile. Mathematically, this last requirement is a constraint that reduces

Table 2
Best adsorption isotherm parameters.

Parameter	(*R*)-Naproxen	(*S*)-Naproxen
q_1^*, mM	465 ± 8	284 ± 2
q_2^*, mM	0.28 ± 0.02	3.9 ± 0.2
0.01 CH_3COOH		
b_1, mM^{-1}	0.0054 ± 0.0001	0.0146 ± 0.0001
I	0.34 ± 0.04	
b_2, mM^{-1}	0.25 ± 0.07	0.133 ± 0.006
0.01 CH_3COOH–0.01 CH_3COONH_4		
b_1, mM^{-1}	0.0065 ± 0.0001	0.0181 ± 0.0002
I	1.13 ± 0.06	
b_2, mM^{-1}	0.08 ± 0.11	0.039 ± 0.005
0.03 CH_3COOH–0.03 CH_3COONH_4		
b_1, mM^{-1}	0.0067 ± 0.0001	0.0174 ± 0.0001
I	0.67 ± 0.03	
b_2, mM^{-1}	6.4 ± 0.5	0.236 ± 0.009

the number of independently adjustable parameters for each profile by two, resulting in a more robust solution. It is worth to note that the adsorption isotherms drawn using the data in Table 2 are in a good agreement with those determined by the Glueckauf method. Consequently, the latter method provides trustworthy results when used to study the adsorption of ionized compounds.

4.2.2. Analysis of the selected model

The adsorption equilibrium model proposed in Eqs. (24) and (25) agrees in major points with earlier findings [21,23]. This model assumes the coexistence of two groups of adsorption sites: numerous sites of relatively low affinity and sparse sites of relatively high affinity toward Naproxen. It also implies somewhat different mechanisms of adsorption for the two enantiomers. Differences in the adsorption models used in the present and in previous works arise from the fact that this new study encompasses a wider range of buffer compositions and solute concentrations. To better take into account new phenomena, e.g., dissociation and ion–ion interactions, more sophisticated models are necessary. A concept used earlier to describe enantioselective adsorption [21,23] can be thought as a particular case of the more general model presented here. This model assumes localized adsorption for the more strongly retained enantiomer and adsorption, probably nonlocalized and certainly allowing adsorbate–adsorbate interactions, for the less retained one. This can be explained since enantioselectivity implies strong binding of the preferentially adsorbed enantiomer inside the chiral cleft of a selector moiety whereas its optical antipode can adsorb only on the external surface of the chiral selector, where it is available for interactions with neighbor molecules. This interpretation is supported by a comparison between the total saturation capacities of the two enantiomers. The ratio $q^*(R)/q^*(S)$ is equal to ca. 1.6 suggesting nonstoichiometric adsorption of (*R*)-Naproxen. The situation is easy to image if we assume that, when it is adsorbed on a chiral site, the more strongly favored enantiomer prevents other solute molecules from adsorbing on the same site by blocking the functional groups of the selector. In contrast, the unfavored enantiomer retained by nonselective interactions does not block completely the chiral selector functional groups nor involves all its functional groups for binding to this site. The situation is schematically illustrated in Fig. 7.

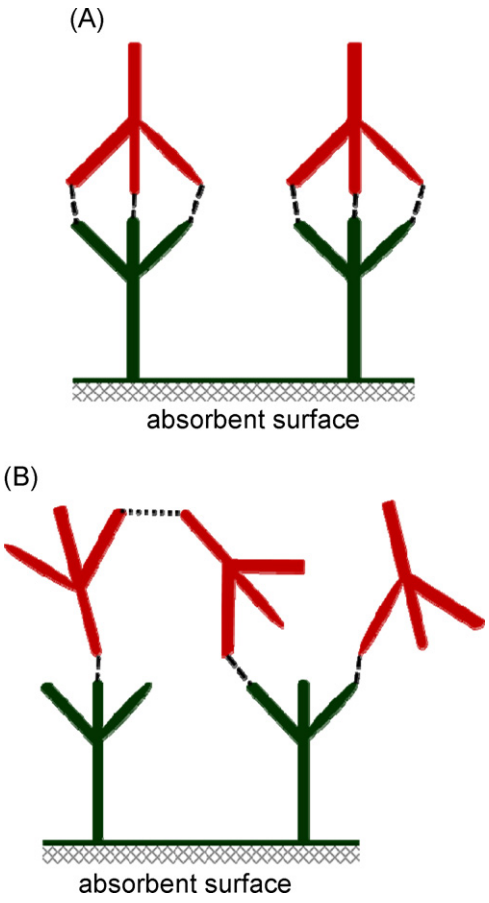

Fig. 7. Illustration of proposed mechanisms for the adsorption of the preferentially retained enantiomer (a) and its antipode (b). Green figures represent the chiral selectors, red figures represent the analyte molecules. Dotted line in scheme (b) symbolizes adsorbate–adsorbate interaction that can be either attractive or repulsive. Note that these schemes serve to illustrate different adsorption mechanisms only for the low-energy enantioselective sites. (For interpretation of the references to color in this figure legend, the reader is referred to the web version of the article.)

Data in Table 2 show that both the high-energy and the low-energy adsorption sites are enantioselective. Moreover the surface densities of these sites differ for the enantiomers. Regarding a large group of the low-energy adsorption sites, it was explained above supposing stoichiometric and nonstoichiometric adsorption of (*S*)- and (*R*)-Naproxen, respectively. As to the high-energy sites, it may be caused by the lumping of the effects of a few groups of high-energy adsorption sites in a single term (the coexistence of two groups of high-energy sites was proven under similar conditions in Ref. [21]). These effects can become nonresolvable in the multiprofile optimization algorithm due to robustness restrictions.

The effect of the buffer composition on the adsorption isotherms is illustrated by the variations of the equilibrium constants and the Moreau interaction parameters *I*. The high-energy site adsorption affinity changes simbatically for both enantiomers in the following order: AN3 > A1 > AN1. For the low-energy sites, these series are somewhat different for (*R*)- and (*S*)-Naproxen: AN3 ≈ AN1 > A1 and AN1 > AN3 > A1, respectively. Note that these series alone cannot explain relationship between the retention of the solute and the ionic composition of the mobile phase since the model used accounts only for the retention of the neutral form. For example, (*S*)-Naproxen is eluted faster with AN3 eluent than with A1 eluent because a considerable fraction of the solute, which is dissociated, is not retained in the former case. The question arises why the isotherm parameters are affected by the mobile phase composition if the dissociation equilibrium is directly taken into account through the dissociation degree in Eqs. (24) and (25)? In the first approximation, it can be answered that the solvation state of the neutral solute depends on the ionic composition of the liquid phase as well, as does the conformation of chiral selectors.

The order of elution of the enantiomers is determined by the low-energy adsorption sites, obviously, due to their high concentration. In the same time, the high-energy interactions play a significant role in the retention of small concentration samples. This role becomes evident when the retention in the eluents AN1 and AN3 is compared for each enantiomer. In both cases, dilute samples are faster eluted with the AN1 buffer. This is because the b_2 coefficients are low in this mobile phase (the eluotropic series is reversed as the sample concentration increases and the influence of the low-energy sites is becoming dominant). A drastic growth of the b_2 coefficients (by two orders of magnitude for (*R*)-Naproxen) following a rise of the buffer concentration is unlikely to be explained by solvation processes or conformational changes in chiral selectors. Rather it suggests the influence of retention mechanisms unaccounted for in the model, such as anion adsorption in the form of ion-pairs, for instance. That some minor forms of strong adsorption were missed in the model in study is suggested by the fact that peak tailing at relative peak height below 10% could not be predicted perfectly (Fig. 6).

An important distinction between retention of the optical antipodes of Naproxen according to the model in consideration consists in the adsorbate–adsorbate interactions of (*R*)-enantiomer.

The respective interaction parameter *I* fluctuates around unity, thus formally demonstrating both repulsive and attractive interactions depending on mobile phase composition. It is hard to explain without speculation why adsorbed molecules interact repulsively in A1 and AN3 buffers but interact attractively in AN1 buffer. Rather one can suppose that the *I* coefficient is an apparent quantity, including along with adsorbate–adsorbate interactions other non-langmurian processes.

5. Conclusion

The adsorption of the Naproxen enantiomers on a Whelk-O1 CSP from buffered methanol–water solutions can be described within the two-site model assuming the independent adsorption of dissociated ions and undissociated molecules. When the methanol percentage is 80vòl.%. like in this work, the adsorption of the anionic species can be neglected. More sophisticated isotherm equations can be proposed to better suit any particular situation. However, the application of such models over a wide range of buffer compositions is complicated for statistical reasons. The whole set of data on the RP chromatography of Naproxen on Whelk-O1 [20–23] including the present work shows that the enantioselective character of the adsorption is due to the adsorption of the enantiomers following different models, not one single model with different coefficients for the two enantiomers. This observation holds true both in acidic media, where dissociation of the analyte is suppressed and in relatively neutral media, where dissociation is considerable.

The effect of dissociation on the elution of ionizable compound results in a strong distortion of chromatograms. Nevertheless the modified Glueckauf method can be used to determine the adsorption isotherms under such conditions. The accuracy of the results so obtained appears to be similar to the accuracy of the inverse method.

Acknowledgments

This work was supported by grant CHE-06-08659 of the National Science Foundation and by the cooperative agreement between the University of Tennessee and the Oak Ridge National Laboratory. L.A. appreciates the support of the Russian Foundation for Basic Research (grant 10-03-00048-a). We also thank Ted Szczerba (Regis Technologies, Morton Grove, IL) for fruitful discussion.

References

[1] F. Gritti, G. Guiochon, J. Chromatogr. A 1216 (2009) 63.
[2] F. Gritti, G. Guiochon, J. Chromatogr. A 1216 (2009) 1776.
[3] F. Gritti, G. Guiochon, J. Chromatogr. A 1216 (2009) 3175.
[4] U.D. Neue, K.V. Tran, A. Méndez, P.W. Carr, J. Chromatogr. A 1063 (2005) 35.
[5] U.D. Neue, Ch.H. Phoebe, K.V. Tran, Y.-F. Cheng, Z. Lu, J. Chromatogr. A 925 (2001) 49.
[6] Y.V. Kazakevich, J. Chromatogr. A 1126 (2006) 232.
[7] C.B. Amphlett, Inorganic Ion Exchangers, Elsevier, Amsterdam, 1964.
[8] B.J. Bennett, F.G. Helerich, Ion Exchange Technology, Horwood, Chichester, UK, 1984, p. 322.
[9] J.S. Pérez, D. Frey, Biotechnol. Prog. 21 (2005) 902.
[10] Cs. Horvath, W. Melander, I. Molnar, Anal. Chem. 48 (1977) 142.
[11] T. Fornstedt, P. Sajonz, G. Guiochon, J. Am. Chem. Soc. 119 (1997) 1254.
[12] G. Götmar, T. Fornstedt, M. Andersson, G. Guiochon, J. Chromatogr. A 905 (2001) 3.
[13] J. Zheng, S.A. Shamsi, J. Chromatogr. A 1005 (2003) 177.
[14] M. Lämmerhofer, W. Lindner, J. Chromatogr. A 741 (1996) 33.
[15] G. Götmar, N.R. Albareda, T. Fornstedt, Anal. Chem. 74 (2002) 2950.
[16] W.H. Pirkle, Ch.J. Welch, J. Chromatogr. A 683 (1994) 347.
[17] W.H. Pirkle, Ch.J. Welch, Tetrahedron: Asymmetry 5 (1994) 777.
[18] M.E. Koscho, P.L. Spence, W.H. Pirkle, Tetrahedron: Asymmetry 16 (2005) 3147.
[19] C.F. Zhao, S. Diemert, N.M. Cann, J. Chromatogr. A 1216 (2009) 5968.
[20] L. Asnin, F. Gritti, K. Kaczmarski, G. Guiochon, J. Chromatogr. A 1217 (2010) 264.
[21] L. Asnin, G. Guiochon, J. Chromatogr. A 1217 (2010) 2871.
[22] L. Asnin, G. Guiochon, J. Chromatogr. A 1217 (2010) 1709.
[23] L. Asnin, K. Horvath, G. Guiochon, J. Chromatogr. A 1217 (2010) 1320.
[24] M. Moreau, P. Valentin, C. Vidal-Madjar, B. Lin, G. Guiochon, J. Colloid Interface Sci. 141 (1991) 127.
[25] F. Gritti, G. Guiochon, Anal. Chem. 77 (2005) 4257.
[26] F. Gritti, G. Guiochon, Anal. Chem. 77 (2005) 1020.
[27] G. Götmar, L. Asnin, G. Guiochon, J. Chromatogr. A 1059 (2004) 43.
[28] L. Asnin, K. Kaczmarski, A. Felinger, F. Gritti, G. Guiochon, J. Chromatogr. A 1101 (2006) 158.
[29] F. Gritti, G. Guiochon, Anal. Chem. 76 (2004) 4779.
[30] Y. Chen, M. Kele, I. Quiñones, B. Sellergren, G. Guiochon, J. Chromatogr. A 927 (2001) 1.
[31] A.N. Frumkin, Z. Phys. 35 (1926) 792.
[32] I. Hägglund, J. Ståhlberg, J. Chromatogr. A 761 (1997) 3.
[33] J. Ståhlberg, J. Chromatogr. A 855 (1999) 3.
[34] E. Bosch, P. Bou, H. Allemann, M. Rosás, Anal. Chem. 68 (1996) 3651.
[35] F.Z. Oumada, C. Ráfols, M. Rosés, E. Bosch, J. Pharm. Sci. 91 (2002) 991.
[36] A. Avdeef, J.E.A. Comer, S.J. Thomson, Anal. Chem. 65 (1993) 42.
[37] E.S.L. Romero, M. Reta, C. Ráfols, E. Bosch, J. Pharm. Biomed. Anal. 49 (2009) 923.
[38] F. Gritti, G. Guiochon, Anal. Chem. 81 (2009) 9871.
[39] R. Bates, Determination of pH. Theory and Practice, John Wiley and Sons, New York, 1964.
[40] I. Canals, F.Z. Oumada, M. Roseś, E. Bosch, J. Chromatogr. A 911 (2001) 191.
[41] J.H. Knox, R. Kaliszan, J. Chromatogr. 349 (1985) 211.
[42] J.A. Jönsson, P. Lövkvist, J. Chromatogr. 406 (1987) 1.
[43] S.N. Lanin, M.Yu. Ledenkova, S.Yu. Nikitin, Mendeleev Commun. 10 (2000) 37.
[44] G. Guiochon, A. Felinger, A.M. Katti, S.G. Shirazi, Fundamentals of Preparative and Nonlinear Chromatography, 2nd ed., Academic Press, Boston, MA, 2006.
[45] F. Gritti, G. Guiochon, J. Chromatogr. A 1003 (2003) 43.
[46] L. Asnin, K. Kaczmarski, G. Guiochon, J. Chromatogr. A 1138 (2007) 158.
[47] P.V. Danckwerts, Chem. Eng. Sci. 2 (1953) 1.
[48] K. Kaczmarski, J. Chromatogr. A 1176 (2007) 57.
[49] J.C. Nash, Compact Numerical Methods for Computers: Linear Algebra and Function 583 Minimisation, Adam Hilger, Bristol, 1990, p. 215.
[50] F. Gritti, G. Guiochon, J. Chromatogr. A 1216 (2009) 8874.
[51] A. Seidel-Morgenstern, J. Chromatogr. A 1037 (2004) 255.